Research Open

Microbiology, Immunology and Pathology

Volume 5 Issue 2

Research Article

Pheromonicin: A Novel Antimicrobial Inhibited Fatal Multidrug-Resistant *M. tuberculosis* Infection in Animal Models

Xiao-Qing Qiu[1*], Ke-Fu Cao[1†], Zhi-Hong Xiong[2†], Xiao-Feng Zhang[1†], Yu Pang[6†], Chong-Yi Tong[1], Carolyn Shoen[3], Xiao-Dong Han[4], Guo-Kun Ao[4], Rong-Qi Li[1], Salmaan Keshavjee[5], Yu Wang[6], Yan-Lin Zhao[6] and Michael Cynamon[3]

[1]Laboratory of Biomembrane & Membrane Proteins, West China Hospital, Sichuan University, Chengdu, China

[2]Institute of Tuberculosis Research, 309 Hospital, Beijing, China

[3]VA Medical Center and SUNY Upstate Medical University, Syracuse, USA

[4]Department of Radiology, 309 Hospital, Beijing, China

[5]Department of Global Health and Social Medicine, Harvard Medical School, Boston, USA

[6]National Tuberculosis Conference Laboratory, China Centers for Disease Control, Beijing, China

[†]Authors have the equivalent contribution

Corresponding author: Xiao-Qing Qiu, Laboratory of Biomembrane & Membrane Proteins, West China Hospital, Sichuan University, Chengdu, Sichuan, China

Received: November 26, 2024; **Accepted:** December 02, 2024; **Published:** December 09, 2024

Abstract

There is an urgent need for effective new drugs to combat multidrug-resistant *M. tuberculosis* (MDR-TB). We found the outer membrane porin A of MDR-TB (OmpATb), a member of the OmpA family which shares epitopes with a variety of microbes, could be targeted by a 28-residue antibody mimetic by fusing two antibody Fab complementarity-determining regions (VHCDR1 and VLCDR3) through a cognate framework region (VHFR2) of a monoclonal antibody which recognizes OmpA of N. meningitidis. We constructed a fusion protein, pheromonicin-NM (PMC-NM), by linking colicin Ia, a bactericidal molecule produced by *E. coli* which kills target cells by forming a voltage-dependent channel in target cell membrane, to that antibody mimetic. The OmpATb/antibody mimetic interaction initiated the formation of irreversible PMC-NM channel in MDR-TB cell membrane resulting in leakage of cellular contents. PMC-NM demonstrates high efficacy, 103-5 times greater than that of current anti-TB agents, against 506 isolates of MDR-TB. It can reduce pulmonary TB CFU 2-3 logs compared to controls in murine TB models. With a 22-wk PMC-NM treatment, 75% macaques survived MDR-TB infection that was lethal to untreated and INH/RIF-treated controls. No relapse occurred in the subsequent 26-wk observation period for 60% of the macaques. PMC-NM significantly altered outcomes of *in vivo* fatal MDR-TB infection without evident toxicity, making it an appropriate candidate for further clinical evaluation.

Keywords: *OmpATb, Guidance of antibody mimetic, Cellular leakage, Intracellular clearance, Pulmonary TB burdens, Clinical outcomes*

Introduction

Tuberculosis (TB) is the biggest infectious killer of adults, causing approximately 1.8 million deaths and 10.4 million new cases each year [1-4]. Multidrug-resistant tuberculosis (MDR-TB), caused by strains of Mycobacterium tuberculosis resistant to at least isoniazid (INH) and rifampicin (RIF), the backbone of the current empirical first-line anti-tuberculosis regimen, affects an estimated 600,000 people every year. Cases of extensively drug- resistant tuberculosis (XDR-TB), resistant to INH/RIF, fluoroquinolone, and amikacin, capreomycin or kanamycin, have been observed worldwide, most notably in high burden countries such as China, India, throughout Africa, and Eastern Europe [1-4]. Current therapies for drug-resistant tuberculosis offer a very low cure rate – roughly 50 percent – and therapy ranges from 9 months to two years, therefore, new drugs are urgently needed to combat MDR/XDR-TB infections [4].

Outer membrane porin A of *M. tuberculosis* (OmpATb), located on the outer membrane of Mtb cells [5-8], could serve as a potential target for new drugs. We postulated that OmpATb might appear on the surface of infected host cells [9,10] If that was the case, the new drug would be able to kill both Mtb cells and infected host cells.

As an example of channel-forming bacteriocins, colicin Ia, a typical E1 family colicin, is bactericidal to *E. coli* and might be able to be developed as a novel candidate against MDR-TB infection, if the native targeting ability of wild-type colicin Ia could be altered. Colicin Ia kills target cells by forming a voltage-activated channel in the target cell membrane via its 175-residue C-terminal channel-forming domain [11-16]. It acts on the lipid bilayer of cell membranes, therefore, colicin Ia could be engineered for insertion into the cell membrane of bacteria that are not its natural targets [18]. In target cell membrane, the active form of colicin Ia is a monomer [12-16].

To target the channel-forming domain of colicin Ia to the cell membrane of other bacteria, we initially constructed fusion proteins

consisting of either an 8-residue staphylococcal AgrD1 pheromone, or a 7-residue enterococcal cCF-10 pheromone, or a 13-residue Candida a-factor pheromone fused to the channel-forming domain of colicin Ia. The fusion proteins demonstrated effective bactericidal activities against methicillin- resistant Staphylococcus aureus, or vancomycin-resistant Enterococcus faecalis, or Candida albicans *in vitro* and *in vivo*, respectively [17-19]. We then selected certain antibody complementarity-determining regions (CDRs) and framework region sequences to create a single-chain antibody mimetic comprising two interacting V_H- and V_L-derived CDRs. The mimetic retains the basic antigen-recognition ability of the whole parent antibody and acts as a smaller, proper-affinity binder [20]. We previously found that the most promising structure comprises V_HCDR1 and V_LCDR3 connected by a corresponding V_HFR2 sequence, forming a 28-residue antibody mimetic [20].

Materials and Methods

Construction and Purification of Pheromonicin-NM

The antibody mimetic amino acid sequence was constructed to follow position I626 of colicin Ia by double-stranded mutagenesis (Quick Change kit, Strategene) using a pET-11 plasmid containing the colicin Ia gene to form pheromonicin-NM (PMC-NM). The oligonucleotide used, containing the desired SYWLHWIKQRPGQGLEWIGSQS

THVPRT mutation, was 5'-GCG AAT AAG TTC TGG GGT ATT TCT TAT TGG CTG CAT TGG ATT AAA CAG TAA ATA AAA TAT AAG ACA GGC-3', 5'-TGG CTG CAT TGG ATT AAA CAG AGA CCT GGT CAG GGA CTG GAA TGG ATA TAA ATA AAA TAT AAG ACA GGC-3' and 5'- GGT CAG GGA CTG GAA TGG ATA GGA TCT CAG TCC ACG CAT GTG CCG AGA ACC TAA ATA AAA TAT AAG ACA GGC-3'. The harvested plasmid was transfected into pET BL-21 (DE3) *E. coli* cells to produce PMC-NM as previously described10-13. As determined from 12% SDS-polyacrylamide gel assays, PMC-NM eluted by 0.3 M NaCl comprised about 90% of total eluted protein (Figure 1d).

Amino acid Sequences of Mimetics of Other Tested Pheromonicins

The sequences of the V_HCDR1-V_HFR2-V_LCDR3 of the following parent molecules are:

HB8627 IgM recognized non-small cell lung cancer:

DYYLHWVKQRTEQGLEWIGQHIRELTRS

IgG recognized *B. dendrobatidis*: GYTMEWVKQSHGKN-LEWIGQNGNTLPYT

AF468835 recombinant single chain Fv Ab recognized *N. gonorrhoeae*:

TYAMNWVRQAPGKGLEWVAQQGQSYPLT

IgG recognized *Cyanobacteria*: SYWMQWVKQRPGQGLEWIGQ-QYWSTPPWT

MDR-TB Isolates Used for *In vitro* and *In vivo* Rodent and Primate Infection

506 clinical isolates of MDR-TB were collected by China CDC from southern and western China with 10% XDR-TB isolates for *in vitro* study. Mtb Erdman, H37Rv, MDR-06005 and PUMC-94789 were used for rodent and primate infection models in the present study. MDR-06005 is a Beijing genotype strain that is katG 315 and gyrA 281 genetic mutations (isolated by Institute of Tuberculosis Research, 309 Hospital, Beijing). PUMC-94789 is a Beijing genotype strain that is with katG 315, rpoB 531, 526 and gyrA 94 genetic mutations, and presented a 7-d median death time in mice test (isolated by Institute of Experimental Animal Sciences, Peking Union Medical College).

Minimum Inhibition Concentration

100 µl of double-diluted preparations of either PMC-NM, INH, or other routine anti-TB agents was added into respective wells of 96-well plate while only 100 µl 7H9-S broth was added into the control well, then 100 µl of inoculum (TB cells, 10^6CFU/ml in 7H9-S broth) was added into each well. The plates were sealed in plastic bags and incubated 10 days (37°C) after inoculation. The lowest concentration of each agent which prevented the visual growth of Mtb cells was interpreted as MIC. MIC measurement of PMC-NM against isolates of Gram-positive and -negative Omp A bacterium were performed at Antibiotic Division, National Inst. for Food and Drug Control. China FDA with a paid service contract. Incubation time was 12-24 hrs (37°C) after inoculation.

In vitro Inhibition Test

100 µl of preparations of PMC-NM, or INH, or wild-type colicin Ia, or Rev-PMC-NM was added into respective wells of 96-well plate while only 100 µl 7H9-S broth was added into the control well, then 100 µl of inoculum (H37Rv cells, 10^6CFU/ml in 7H9-S broth) was added into each well. The plates were sealed in plastic bags and incubated 2, 3, 7, 8 days (37°C) after inoculation. Turbidometric absorbance of each well was measured.

Phase I incubation test, 3 ml 7H9 solution inoculated with H37Rv (0.1 ml, 10^{4-5} CFU), treated with (1) 50 mM borate buffer (colicin Ia and PMC-NM stock solution), (2) 1 ug/ml wild-type colicin Ia, (3) 1 ug/ml PMC-NM, incubated at 37°C for 6 weeks.

Phase II incubation test, 3 ml 7H9 solution inoculated with H37Rv, treated with (1) nothing, (2) 50 mM borate buffer, (3) 2 ug/ml wild-type colicin Ia, (4) no inoculation but remains of phase I PMC-NM treatment culture (3,000 rpm centrifuged 10 min), incubated at 37°C for 10 weeks.

Bifidobacterium longum (1.2186) and *Lactococcus lactis* (1.2472) (Inst. Microbiology, China Academy of Science) (50 µl, 10^{3-4} CFU/ml) was smeared on the surface of respective solid medium with PMC-NM and ampicillin treatments, incubated 18 hrs (37°C).

Rodent *In vivo* Bactericidal Activity

Female BALB/C mice (six per group) were infected intranasally with 6.8 x 10^2 CFU of Mtb Erdman (ATCC35801). Twenty-one days post-infection mice were treated with either intraperitoneal injection (i.p.) of saline, or PMC-NM 20 or 40 mg/kg/d, or oral delivery of INH 25 mg/kg/d for 4 weeks. Right lungs were collected for Mtb CFU determination.

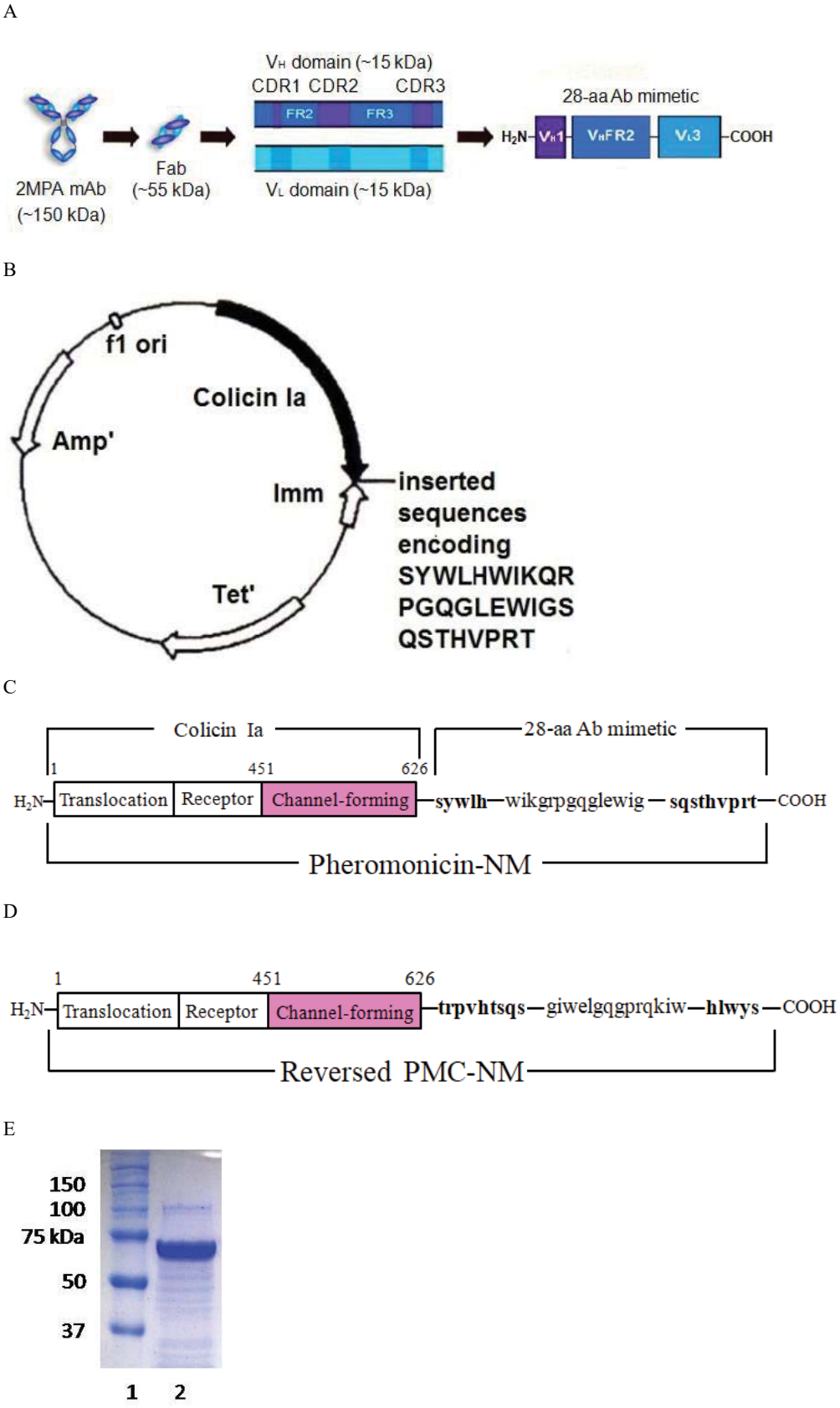

Figure 1: Structure and *in vitro* bioactivity of PMC-NM.

(**A**) Structure of the antibody mimetic comprising the V_HCDR1, V_HFR2, V_LCDR3 domains of Fab of 2MPA mAb. (**B**) 8.3 kbp colicin Ia plasmid used for site-directed mutagenesis of colicin Ia gene to insert the gene encoding the antibody mimetic. (**C**) A domain diagram of the PMC-NM. (**D**) The Rev-PMC-NM constructed with scramble mimetic. (**E**) PMC-NM (70 kDa) comprised about 90% of total SDS eluted protein. Lanes, (1) marker, (2) PMC-NM.

Female BALB/C mice were injected with 0.2 ml 105-6 CFU/ml of MDR06005 MDR-TB strain through the tail vein. Three days after infection, mice were randomly assigned into four treatment groups (twenty per group) and i.p. with 0.9% saline alone, INH 6, or 12, or 27 mg/kg/d, PMC-NM 5, 10, or 20 mg/kg/d daily for 4 -weeks. The number of surviving animals at various time points was determined. Kaplan-Meier analysis was used to determine the significance of differences between the PMC-NM and control groups. All *in vivo* protocols were approved by the Institutional Animal Care and Use Committee of Sichuan University and Project of Sichuan Animal Experimental Committee, License 045, Institutional Animal Care and Use Committee of China CDC and Project of Beijing Animal Experiment Committee, license CNAS BL0047, China, and Subcommittee for Animal Safety, VAMC, Syracuse, NY.

Immunolabeling Assay

Pheromonicin-NM was injected i.p. into mice, or macaques that had been infected with MDR-TB cells 4-6 weeks (mice), or 17 weeks (macaque) prior. The animals were killed 12-24 hrs after injection, and the lungs were fixed for formalin and paraffin-embedded prior to sectioning. Sections were sealed with 5% BSA, and then incubated with anti-OmpA (rabbit IgG, MyBioSource, San Diego, USA), or anti-pheromonicin (mouse, AbMax, Beijing) antibodies for 30 min. at 37°C, washed and incubated with FITC- anti-rabbit and rhodamine-anti-mouse goat antibodies (Bioss, Beijing) for 15 min. at 37°C, and washed. The sections were examined under an optical/fluorescent microscope (Nikon 90i) with DM400, DM505 and DM565 filters.

MDR-TB infected macaque lung tissues were fixed with 2.5% paraformaldehyde, dehydrated with gradient concentrations of ethyl alcohol, embedded in gelatin, and sectioned with Leica EM UC6 ultramicrotome, ultra-thin sections were probed with above rabbit anti-OmpA Ab and mouse anti-pheromonicin Ab as first Ab, 2nd Ab were goat anti-rabbit 5 nm colloidal gold and goat anti-mouse 10 nm colloidal gold IgGs, (Sigma), stained with uranyl acetate and observed under a transmission electron microscope (Hitachi HT7700, Japan).

Immunoblotting Assay

Pellets of H37Rv Mtb strain (2 gm) and macaque lung tissues (2 gm, extracted from autopsy as CFU counting collection) were homogenized, suspended with extract solution A (9 ml with 1: 250 extract sol. C), sonicated for 1hr at 2-8°C, centrifuged 10,000g, 5 min at 2-8°C, supernate suspended with 1: 30 extract solution B, 37°C bathing for 10 min, centrifuged 1,000g, 3 min at 37°C, the thick liquid (bottom layer of layered centrifugation) blended with 1: 1 extract sol. B (membrane protein extraction kit, BestBio, Shanghai). 60 ug preps per well, SDS-10% PAGE electrophoretic transferred to nitrocellulose membrane, incubated with, or without 10 ug/ml PMC-NM, or other tested pheromonicins for 1 hr, 20°C, then 4°C over night, the resulting material were probed with anti-pheromonicin Ab and appropriate secondary antibodies (AbMax, Beijing).

Ethics Statement

The work described in this study was carried out at Center for Primate Biomedical Research, University of Illinois College of Medicine, Chicago and Institute of Experimental Sciences, Peking Union Medical College via paid service contracts, and the Veterans Affairs medical center, Syracuse, NY). All animals were housed in the Animal Bio-Safety Level III (ABSL-III) facility located at Biologic Resources Laboratory, University of Illinois at Chicago and Institute of Laboratory Animal Science, Peking Union Medical College. The housing and animal care procedures were in compliance with the Chinese guidelines for animal experiments (Laboratory animal Requirements of environment and housing facilities GB 14925–2010, China; Regulations on administration of laboratory animals, Ministry of Science and Technology, 1988, China) and with the 8th Guide for the Care and Use of Laboratory Animals of Association (National Research Council, 2011). The animal housing and care procedures were in compliance with the United States Department of Agriculture (USDA) through the Animal and Plant Health Inspection Service under the Animal Welfare Act (AWA). The ABSL-III facility was certified by USDA and Association for Assessment and Accreditation of Laboratory Animal Care (AAALAC) prior to initiation of this project. Office of Animal Care and Institutional Biosafety (OACIB) of University of Illinois at Chicago approved all the study protocols and procedures before this project begins. The approval numbers were: IBC#12-089; ACC#12-210. The ABSL-III Laboratory is certified by the Association for Assessment and Accreditation of Laboratory Animal Care International (AAALAC International). Institutional Animal Care and Use Committee of Peking Union Medical College approved study protocols and procedures prior to starting this project (ILAS-PC-2014-009). Animal protocols were approved by the Subcommittee for Animal Studies (SAS), Veterans Affairs Medical Center, Syracuse, NY. Animals were individually housed in stainless steel wire-bottomed cages (80×80×80 cm3) with sufficient space supplied with a commercial monkey diet and water and twice daily with fresh fruit in an air-conditioned room and monitored by a computer-based system. After infection, animals were also monitored twice daily by experienced staff. Animal health was monitored daily by the animal care and veterinary personnel. Pre-defined humane endpoints including depressed or withdrawn behavior, abnormal respiration rates, serious loss of appetite, severe body weight loss and severe abnormal radiographic changes were applied to reduce discomfort in this study. Serious loss of appetite was defined as no food intake during at least two meals. Severe body weight loss was defined as a 20% weight loss in three consecutive weeks compared to the body weight before TB infection. Animals were euthanized by anesthesia with ketamine (i.m. 3〜5 mg/kg).

Study Plans

Cynomolgus macaques (*Macacca fasicularis*) were infected with MDR-TB PUMC-94789 via bronchoscope and monitored clinically, as previous described. Upon development of active TB, animals were randomly assigned to one of three groups: untreated, combind INH/RIF, or PMN-NM. Animals were followed for 22-wk treatment and subsequent 26-wk observation period. Gross pathology, overall bacterial burden scores, and lung CFU were calculated as described for treatment response. CT scans were performed (a) before infection as the baseline background, (b) day 22 after infection to confirm infection, (c) at time points of 22-wk treatment and subsequent 26-wk observation period

and (d) at the end of treatment or termination of animal. Cynomolgus macaques were infected with *M. tuberculosis* H37Rv via bronchoscope and underwent clinical observation, necropsy and histology.

Clinical Observation, Necropsy and Histopathology

Clinical assessments included body weight, respiratory distress, general alertness/activities and food uptake. Clinical lab tests included CBC, differentials, calculation of total lymphocyte population and serum biochemical examination. Extensive quantification of gross TB lesions in each lung lobe, hilar lymph nodes, pleural and extra thoracic organs was undertaken. Histopathology of TB lesions from right caudal lobe (infection site) and other lobes, chest lymph nodes, and extra thoracic organ/tissues was evaluated.

Tissue Bacterial Burden Measurement

Lung samples (4-5 gm) were collected at necropsy from upper, middle and caudal lobes of left and right lungs. Samples were homogenized with a grinder, and digested in N-acetyl-L-cysteine-NaOH-Na citrate (1.5% final concentration) for 15 min at room temperature, neutralized with phosphate-buffered saline (PBS, 67 mM, pH=7.4) and centrifuged at 4,000 g for 15 min. Sediments were re-suspended with 2 ml PBS buffer. 100 µl of each 10-fold serial dilution was inoculated on 7H11 agar plate, and then incubated at 37°C for 4 weeks. The bacteria burden was calculated according to the number of CFUs on the agar plate.

CFU of organ (lung) was calculated as, [CFU number of agar plate x 10 (10-fold serial dilution)/[weight of sample (mg)/1,000 (gm)]] x weight of lung (gm) CFU/lung

CT Scanning and Abnormal Volume Measurement

Image acquisition. All scans were acquired with a 16-section CT scanner (µCT S-160 scanner, United Imaging, Shanghai) by using a spiral mode with 16 × 0.9375-mm collimation. Exposure settings were 140 kVp and 200 mA. Transverse images were reconstructed at a thickness of 1.0 mm and a 1.0-mm increment by using a moderately soft reconstruction kernel, the smallest field of view that included the outer rib margins at the widest dimension of the thorax, and a 1024 × 1024 matrix. All images were interpreted by radiologists who were blind to the identity of the subject. Semi automated measurements of Pulmonary Abnormal Volume (PAV). Data were transferred from the CT scanner to a digital workstation (United Imaging, Shanghai) with commercially available software for semi-automated PAV measurements (Lung lesions; Tissue Management). Lesions were identified by using transverse thin-slab Maximum Intensity Projections (MIP) that were displayed with window width and level settings of 1500 and −500 HU, respectively. With the candidate lesion was marked, the program automatically looked for adjacent structures which matched conditions around the lesion, started volume measurement by using volume-rendered with the structure and the volume of segmented lesion was calculated. The CT scan which taken before TB infection was used as the baseline.

Statistical Analysis

Comparison of data among experimental groups were performed by t test. Comparison of cumulative survival among experimental groups were performed by Kaplan-Meier analysis. P values of <0.05 were considered to be statistically significant. The following inclusion criteria were used to select macaques: no infectious or chronic diseases, good appetite and behavior, age 2-4 yrs, bodyweight 4-6 kg. The macaques were individually housed in cages for five weeks before pulmonary MDR-TB infection. Three weeks after infection with confirmation of eyelid tuberculin test and pulmonary CT scan, animals were randomly allocated into three treatment groups according to a Blocked Randomization Method.

The sample size was estimated according to following assumption: Group I (placebo control) and Group II (traditional medications control) would have an effect of survivor rate equal to 0%, respectively. Group III (PMC-NM) would be a 50% of survivor rate after a 22-wk treatment intervention (25-wk pulmonary infection). When we combined Group I and Group II into a control group to conduct difference comparing of two survivor rates (0% and 50%) between control group (8 animals) and experiment group (8 animals), and defining alpha=0.05, beta=0.2, a Fisher exact test P value=0.038 under selecting n1=8 and n2=8.

Data from our study showed that the survivor rate of PMN-NM treated group was 75% (6/8,) and the survivor rate of control and traditional medications group was 0% (0/4, 0/4), a Fisher exact test P value=0.030 (one-side), it indicated significant statistical difference. The numbers of surviving animals at various time points were determined, and Kaplan-Meier analysis showed a significant difference between the control and PMC-NM treated group (p=0.003). Therefore, we assume that the sample sizes of our study are sufficient.

Results

PMC-NM demonstrated high efficacy against pan-susceptible and MDR-TB strains under the guidance of 28-residue antibody mimetic.

We fused the antibody mimetic at the C-terminus of colicin Ia to construct colicin Ia-antibody mimetic fusion proteins (Figure 1A-E). The targeting domain in one of them is a mimetic of a mAb (NCBI 2MPA) that recognizes the OmpA of *N. meningitides*, a member of the OmpA family which shares epitopes with over 600 other microbes, including Gram negatives (*E. coli*, *K. peumoniae, E. cloacae, Y. pestis, V. cholerae*) and Gram positives including *M. tuberculosis* (Mtb) [5-8,21]. This porin A-specific antimicrobial fusion protein was named pheromonicin-NM (PMC-NM). Interestingly, PMC-NM does not inhibit the growth of certain probiotics, e.g., *Bifidobacterium longum* and *Lactococcus lactis*, presumably due to their lack of similar OmpA analogs on their surface (Figure S3A).

Among several tested pheromonicins with relevant antibody mimetics derived from antibodies targeting different epitopes, only the PMC-NM interacted with OmpATb of Mtb (Figure 1F). PMC-NM inhibited the growth of OmpA pathogens as a bactericidal agent (Figure 1G) [17,18]. In contrast, significant differences regarding *in vitro* activity indicated that neither wild-type colicin Ia, nor reversed PMC-NM with a scramble mimetic, is be able to target Mtb cells (Figure 1G).

The results of two-phases Mtb growth inhibition showed that phase I (6-wk), PMC-NM (1 ug/ml) inhibited the growth of H37Rv cells while wild-type colicin Ia (1 ug/ml) failed; phase II (10-wk), wild-type colicin Ia (2 ug/ml) still did not inhibit the growth of H37Rv cells. Interestingly, in the phase II tube which was inoculated with remains of phase I PMC-NM-treatment culture, no H37Rv cells re-grew, suggesting that PMC-NM was bactericidal (Figure 1H).

A Minimum Inhibitory Concentration (MIC) assay of 39 isolates of MDR-TB (collected by China CDC) showed there were significant differences regarding MIC50 and MIC90 among PMC-NM, wild-type colicin Ia and reversed PMC-NM (Table 1).

Above results indicated that only the PMC-NM with constructed NM antibody mimetic with accurate N- to C-terminal sequence could target the Mtb cells.

A MIC assay of several pan-susceptible Mtb strains (Mtb Erdman, Mtb HN878 etc) and 506 clinical isolates of MDR-TB (collected by China CDC from southern/western China with 10% XDR-TB) indicated that the PMC-NM MIC of pan-susceptible Mtb strains were 0.027-0.11 nmol (1.875-3.75 x 10^{-3} μg/ml) and the MIC_{50}/MIC_{90} of MDR-TB isolates was 1.14/143 nmol (0.08/10 μg/ml), which were significantly lower than the MIC_{50}/MIC_{90} of 11 standard anti-TB drugs (Figure1I and Table 2). Considering the differences in molecular weight between PMC-NM (70 kDa) and standard anti-TB agents (≤1 kDa), the inhibitory activity of PMC-NM against pan-susceptible Mtb strains and MDR-TB isolates was approximately 10^{3-5} times greater, on a molar basis, than that of standard anti-TB agents. The inclusion of 10% XDR isolates likely expanded the MIC range of PMC-NM.

PMC-NM suppressed the pulmonary TB burdens and altered the clinical outcomes in murine pan-susceptible/MDR-TB infection.

To evaluate whether PMC-NM suppressed the pulmonary TB burdens and altered the clinical outcomes of murine TB infection, we first tested the PMC-NM efficacy against drug-sensitive Mtb Erdman infection model. We subsequently studied PMC-NM efficacy with a mildly drug-resistant Mtb strain infection model using a short-term (30 days) treatment. Female BALB/C mice (six per group) were infected intranasally with $6.8x10^2$ CFU of Mtb Erdman. Twenty-one days post-infection mice were treated with either intraperitoneal injection (i.p.) of saline, PMC-NM (20 or 40 mg/kg/d), or oral delivery of INH (25 mg/kg/d) for 4 weeks. Right lungs were collected for TB CFU determination. Both INH and PMC-NM treatment significantly reduced TB CFU about 10^{2-3} logs compared to that of controls (Figure 2A).

We tested several doses (5, 10 and 20 mg/kg/d, i.p.) of PMC-NM in female BALB/C mice infected with a fatal inoculum of MDR-TB [MDR-06005, PMC-NM ($_{MIC}$=0.08 μg/ml), INH ($_{MIC}$ > 0.2 μg/ml), levofloxacin ($_{MIC}$=4 μg/ml), and moxifloxacin ($_{MIC}$=2 μg/ml), 0.2 ml

Table 1: MIC (ug/ml) of PM-NM and colicin Ia against 39 isolates of MDR-TB.

Agents	*MIC range*	*MIC_{50}*	*MIC_{90}*	*P value(MIC_{50})*	*P value(MIC_{90})*
PMC-NM	0.08-5	0.08	2.5	_____	_____
Rev-PMC-NM	0.16-＞80	10	＞80	＜0.01	＜0.001
Wild-type colicin Ia	0.625-＞80	10	＞80	＜0.01	＜0.001

Table 2:

MIC (nM (ug/ml)) of agents against 506 isolates of MDR-TB (10% of them were XDR)

Agents	*MIC range*	*MIC_{50}*	*MIC_{90}*	*P value* (MIC_{50})	(MIC_{90})
PMC-NM	**1.14-572** (0.08-40)	**1.14** (0.08)	**143** (10)		
Isoniazid	**460-1.87x10^6** (0.063-256)	**58,400** (8)	**> 9.34x10^5** (>128)	<0.001	<0.001
Rifampicin	**152-1.55x10^5** (0.125-128)	**>38,900** (>32)	**>1.55x10^5** (>128)	<0.001	<0.001
Ethambutol	**612-6.27x10^5** (0.125-128)	**19,600** (4)	**> 6.27x10^5** (>128)	<0.001	<0.001
Capreomycin	**46-48,930** (0.031-32)	**191** (0.125)	**3,058** (2)	<0.05	<0.05
Kanamycin	**64-66,250** (0.031-32)	**2,070** (1)	**8,280** (4)	<0.01	<0.01
Levofloxacin	**84-86,500** (0.031-32)	**1,350** (0.5)	**43,240** (16)	<0.05	<0.001
Amikacin	**53-54,700** (0.031-32)	**427** (0.25)	**3,420** (2)	<0.05	<0.05
Moxifloxacin	**77-79,800** (0.031-32)	**623** (0.25)	**4,984** (2)	<0.05	<0.05
Gatifloxacin	**66-67,800** (0.031-32)	**530** (0.25)	**4,237** (2)	<0.05	<0.05
Linezolid	**92-94,955** (0.031-32)	**5,934** (2)	**23,740** (8)	<0.001	<0.001
Clofazimine	**66-67,650** (0.031-32)	**4,228** (2)	**16,910** (8)	<0.001	<0.001

■ Sensitive ■ Resistant

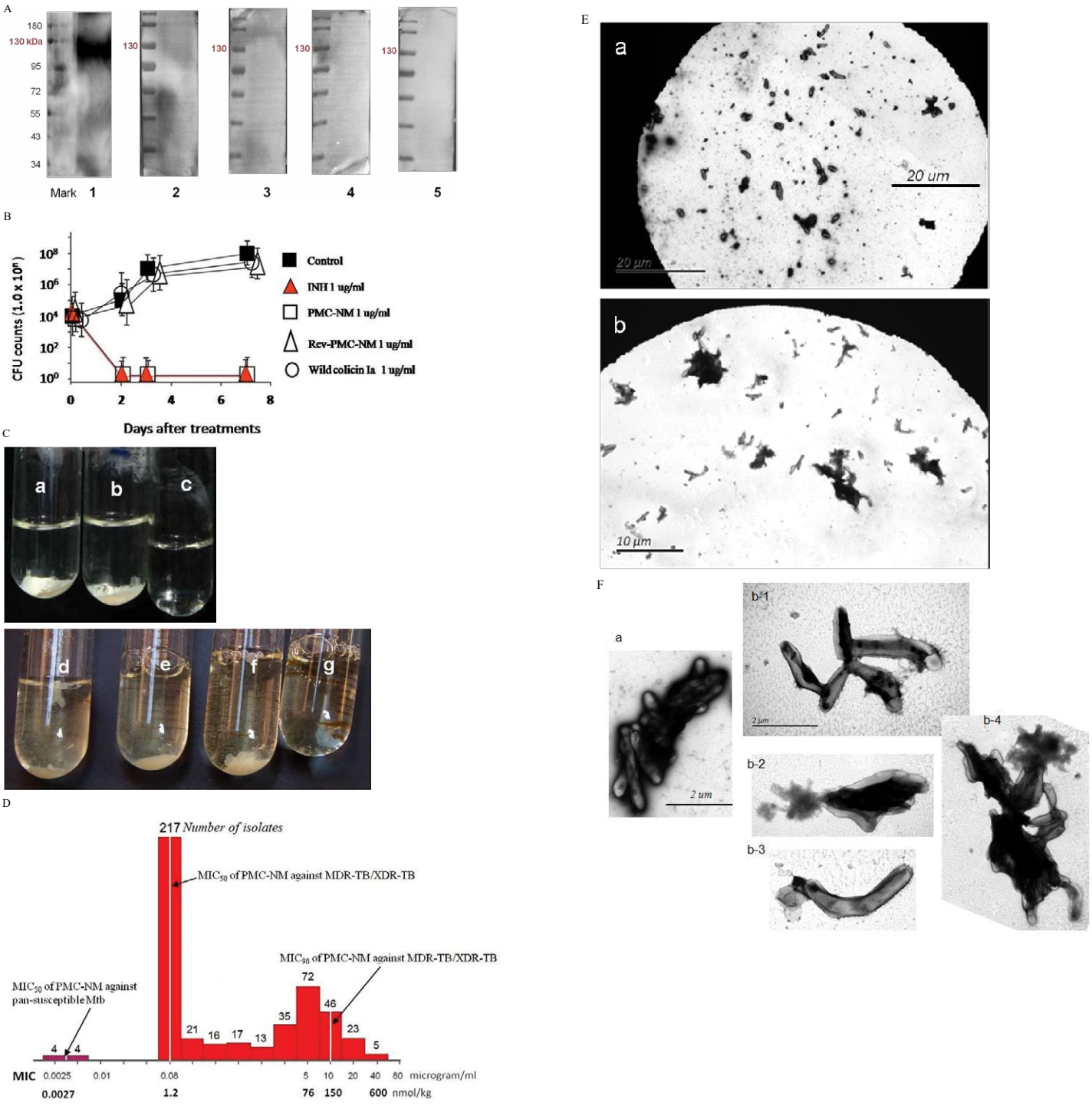

Figure 2: (**A**) Immunoblotting assay showed that only the PMC-NM, not other PMCs, interacted with extracted OmpATb of Mtb H37Rv (about 114 kDa). Lanes, (1) PMC-NM, (2) PMC-*cyanobacteria*, (3) PMC-*B.dendrobatidis*, (4) PMC-HB8627, (5) PMC-*N.gonorrhoeae*. (**B**) PMC-NM inhibited the growth of OmpATb pathogens (Mtb H37Rv) as a bactericidal agent. (**C**) Wild-type colicin Ia could not inhibit but PMC-NM inhibited the growth of H37Rv in the test tube. Phase I (6-wk), all tubes inoculated with H37Rv cells, (a) control, (b) wild-type colicin Ia 1 ug/ml, (c) PMC-NM 1 ug/ml, phase II (17-wk), all tubes inoculated with H37Rv cells, but tube g inoculated with remains of phase I PMC-NM-treated culture. (d) control, (e) spare borate buffer, (f) wild-type colicin Ia 2 ug/ml. (**D**) The MIC frequency distribution of PMC-NM against measured several drug-sensitive Mtb strains and 506 isolates of MDR-TB/XDR-TB. (**E**) After 2 hrs incubation with (**Ea**) INH 1 μg/ml, or (**Eb**) PMC-NM 2 μg/ml, INH did not show any efficacy on MDR-TB cells but PMC-NM killed all MDR-TB cells. Bar, 10 or 20 μm. (**F**) Comparing with normal MDR-TB cells (**Fa**), (**Fb**) Destroyed MDR-TB cells were either ruptured, or shrinkage as empty cell-ghosts with leakage of cellular contents with PMC-NM treatment (2 μg/ml).

10^{5-6} CFU/ml] given through the tail vein. We found that 10 mg/kg/d of PMC-NM yielded a 75-80% survival rate but 5 mg/kg/d of PMC-NM failed (Figure 2B). Subsequently, we selected 10 mg/kg/d as an *in vivo* protective dose against MDR-TB infection for further studies.

The PMC-NM molecules were able to selectively accumulate in the pulmonary TB lesions 1 to 12 hrs after a one-time i.p. application (10 mg/kg) (Figure 2C).

PMC-NM treatments significantly reduced TB burdens and infection levels in macaque pan-susceptible Mtb infection [22-26]. Since primate models are most similar clinically and pathologically to human TB infection, cynomolgus macaques were selected to determine *in vivo* efficacy of PMC-NM. Healthy cynomolgus macaques could tolerate 2-wk PMC-NM treatment with daily intravenous injection (i.v.) as the dose increased from 0.8 to 2 mg/kg/d with no apparent abnormalities.

Sixteen macaques were studied using several regimens to compare 5-wk PMC-NM treatment (i.v. 2 mg/kg/d, n=6) with a saline-treated control group (n=6) and orally dosed INH groups (0.1 mg/kg/d, n=2), or (1.0 mg/kg/d, n=2). Five hundred CFU pan-susceptible H37Rv cells was inoculated into the right caudal lung lobe of each macaque through a bronchoscope. Treatment started at day 24 post -infection. Comparative measurements of TB CFU and pathology scores suggested that PMC-NM treatments significantly reduced TB burdens and pathology score in lung tissues (Figure 2D-E and Figure S1A).

PMC-NM Altered the Clinical Outcomes in Macaque MDR-TB Infection

Pharmacokinetic assays indicated that i.p. application provided a longer circulatory retention contour than that of i.v. application (Figure 3A), therefore, we selected i.p. delivery to yield a longer PMC-NM exposure in pulmonary lesions.

A high virulence MDR-TB isolate [PUMC-94789], PMC-NM ($_{MIC}$=0.08 μg/ml), INH ($_{MIC}$=4 μg/ml), RIF ($_{MIC}$=64 μg/ml), ethambutol ($_{MIC}$=4 μg/ml) was selected to infect macaques (Table 3). Four-wks of PMC-NM treatment (i.p. 3 mg/kg/d, n=4) was compared to untreated controls (n=4)(Figure S1B). Results indicated that (a) 300 CFU of PUMC-94789 cells created a successful infection model, (b) i.p. PMC-NM was efficacious in this model.

Sixteen macaques were infected with 300 CFU of PUMC-94789 cells in the right caudal lung lobe. Infection was confirmed by eyelid tuberculin testing and CT scans 3-wks after inoculation. The animals were randomly allocated into three 22-wk treatment groups: untreated controls (n=4), combined INH/RIF-treated (i.p. 21.8/3.65 μmol/kg/d (3/3 mg/kg/d), n=4, doses adjusted from reported MDR-TB rodent studies) [27,28], and PMC-NM-treated (i.p. 43 nmol/kg/d (3 mg/kg/d), dose adjusted from previous rodent/macaque doses, n=8). Treatment was initiated day 24 post-infection. Seventy-five per cent of PMC-NM-treated group survived. All untreated and INH/RIF-treated controls and two PMC-NM-treated macaques reached the humane endpoint within 10-17 weeks post-infection. All macaques that reached the humane endpoint suffered from clinical symptoms related to MDR-TB infection confirmed at necropsy (Figure 3B, C and Figure S2A-C). Serial CT scans were performed before the infection, and during the entire test period [29,30]. The whole pulmonary TB lesion volume in each CT scan was the summation of lesions in every 1-mm thick digitally dissected CT image (Figure S2A and S2D). The clinical outcome of each macaque was quantitatively extrapolated as the function of serial variation of TB lesion volumes during the entire test period (Figure 3D-F).

The MDR-TB infection in the macaques underwent different clinical courses with respective treatments (Figure 3B-G and Figure S2A-C), (a) all untreated and INH/RIF-treated macaques were euthanized around 10～17-wk post-infection while TB lesion volumes continuously enlarged with pulmonary TB CFU growth (Figure 3Da, Fa); (b) two macaques with low bodyweight (≤ 4 kg) were randomly allocated in the PMC-NM group, we assume that poor physiological conditions might be the reason for the apparent failure of PMC-NM. The lung cultures yielded no growth and decreased TB lesion volumes suggesting control of the TB infection (Figure 3Db, Fb); (c) two PMC-NM-treated macaques were euthanized at 47-wk post-infection with relapsed infection which suppressed by a second 18-wk PMC-NM treatment, presumably their doubled lesion volumes compared to the other PMC-NM treated animals at the end of first

Table 3: Killing rate against Mtb cell/human pulmonary cell culture.

Colony Forming Units							
Group	Day 3					Day 7	
	Conc.2	KR 2	Conc.1	KR 1	Mean of KR	Conc.2	Conc.1
PMC-1ug	75	11.76%	13	65.57%	32.67%	0	0
PMC-10ug	33	61.18%	11	60.71%	60.95%	0	0
INH-1ug	20	76.47%	6	78.57%	77.52%	0	0
Untreated	85	0.00%	28	0.00%	0.00%	0	0
Note	KR(Killing Rate)=(GM-G.exp)/GM						

Note: Conc.2 : Seed 0.5ml-A549/well at $2x10^5$/ml in 24 well flat-plate.
Conc.1 : Seed 0.5ml-A549/well at $1x10^5$/ml in 24 well flat-plate.
Comments:
1. The killing rate as control group, Isoniazid (1ug/ml), reaches 78% on day 3.
2. The killing rate as exp. group, pheromonicin (1ug/ml & 10ug/ml), reaches 33% & 61% respectively on day 3.
3. A549 cells will be apoptotic from on day 3 as critical point under the exp. concentrations.
4. Mtb bacteria die on day 7 with loss of cell host.

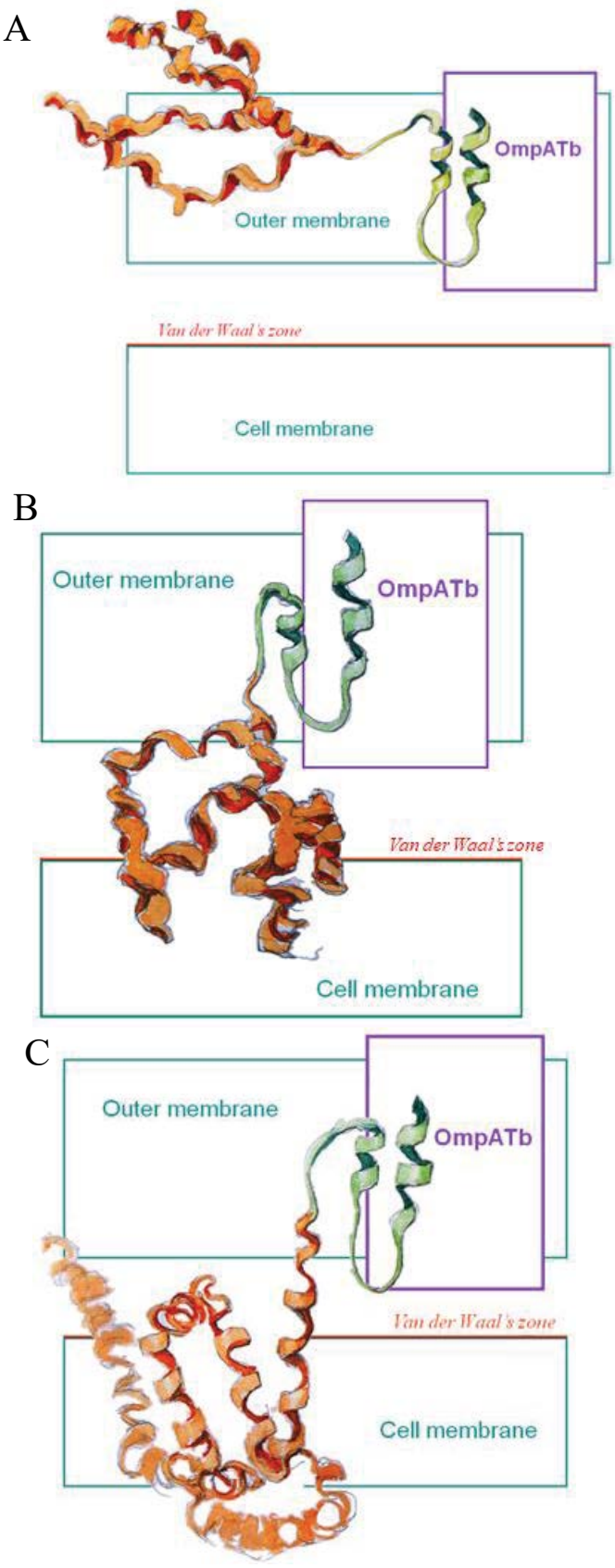

Figure 3: Probably PMC-NM targeting/killing mechanism.

(**A**) Antibody mimetic (green) interacted with OmpATb to drag the channel-forming domain (orange) to bind the cell membrane, (**B**) hydrophobic interaction drove the channel-forming domain to form channel, (**C**) transmembrane potential opened the channel resulting in the leakage of cellular contents.

treatment, facilitated their relapse (Figure 3Ea, Fc); (d) sixty per cent of surviving PMC-treated macaques completed the 52-wk study with no measurable lesion volumes or TB CFU growth but increased their body weight (Figure 3Eb, Fd).

The TB strain which grew in the infected macaque lungs displayed the same resistance profile as the original PUMC-94789 strain (Table 4). The main lesion in untreated primates was acute tuberculosis pneumonia while in INH/RIF-treated primates was granulomas. In contrast, the lesions in PMC-NM-treated primates was significantly less than above groups (Figure 3G,H and Figure S2E).

The serum biochemical data of untreated and PMC-treated monkeys were compared in reference to normal values (Table 5), The BUN/CRE of PMC-treated were in normal range but that of untreated were upper limit of normal or above ; the GLU and TG values of untreated were low, the CK and LDH of untreated were almost 10 times higher than upper limit of normal indicated there might be some muscle/bone and multi-organ TB lesions. Above significant differences between untreated and PMC-treated serum biochemical data indicated that untreated monkeys had serious multi-organ and metabolic abnormalities due to MDR-TB infection, however, PMC protected monkeys with no apparent toxicity.

Table 4:

Selected MDR strain as the pathogen for macaque test

MIC (nM) of agents and LD_{50} toxicity

Agent / *Strain*	RIF	INH	EMB	CP	KN	LF	PMC-NM	LD_{50}
94782	> 7.7×10^4	2.9×10^4	3.9×10^4	670	1,700	2,700	1.14	10d
94789	> 7.7×10^4	2.9×10^4	1.9×10^4	170	3,400	670	1.14	7d
94867	3.9×10^4	1,820	4,900	80	880	340	1.14	12d
94763	> 7.7×10^4	456	1.9×10^4	80	3,400	170	1.14	12d
H37Rv	76	456	4,900	80	860	170	1.14	14d

(a) Red words = resistance to the agent, (b) LD_{50} = Mice survival time with inoculation of LD_{50} dosages of pathogen.

Table 5:

WGS-based SNPs associated with drug resistance in the *M. tuberculosis* isolate from infected macaques

Locus	Mutations of strain 94789			Mutations of strain collected from macaques infected with strain 94789	
	Nucleotide change	Amino acid change		Nucleotide change	Amino acid change
rpoB	CAC→TAC	His526Tyr		CAC→TAC	His526Tyr
	TCG→TTG	Ser531Leu		TCG→TTG	Ser531Leu
katG	AGC→ACC	Ser315Thr		AGC→ACC	Ser315Thr
gyrA	GAC→GGC	Asp94Gly		GAC→GGC	Asp94Gly

The strain isolated from macaques harbored four different amino acid substitutions conferring RIF, INH and FQ resistance, including His526Tyr and Ser531Leu in *rpoB* gene, Ser315Thr in *katG* gene, and Asp94Gly in *gyrA* gene. Above mutation profiles were consistent with those of the PUMC-94789 strain, indicating that TB infections in the animals were induced by the inoculation of PUMC-94789.

Table 6:

No significant difference of liver/kidney functions between PMC-NM treated macaques and untreated macaques

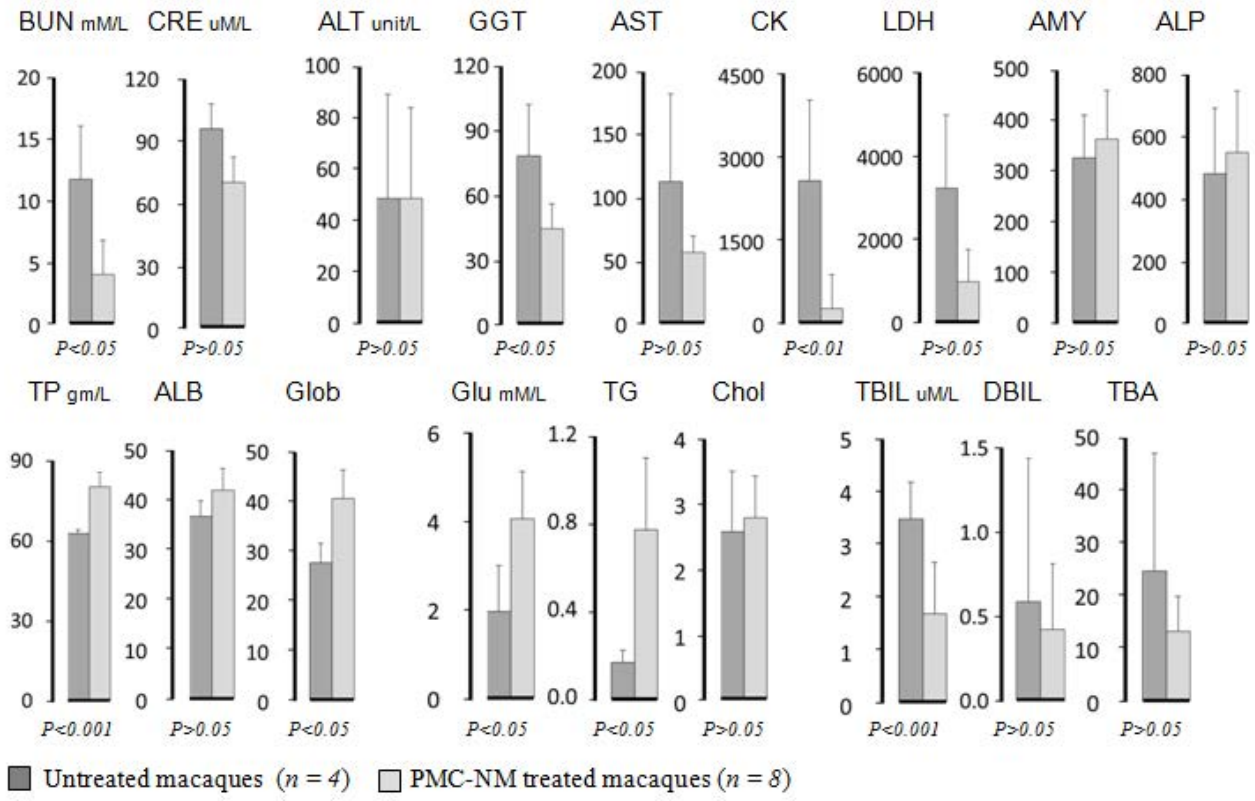

Discussion

Our results indicate that daily PMC-NM treatment (i.p. 43 nM/kg/d for 22-wks), initiated 24 days after fatal MDR-TB infection can significantly reduce MDR-TB lesions in lungs and clinically cure certain cases. To our knowledge, this is the first report of a channel-forming toxin-antibody mimetic fusion protein altering the clinical course in fatal MDR-TB infected rodent and primate models.

Several findings suggested the antibody mimetic domain of PMC-NM molecules targeted the OmpATb appearing on the surface of either Mtb cells, or infected host cells with internalized Mtb cells [5-10,31-35]; (a) immunoblotting data showed only PMC-NM with 28-residue antibody mimetic of 2MPA mAb, not other tested pheromonicins, interacted with OmpATb (Figure 1f), (b) Growth inhibition data demonstrated that without fused 28-residue VHCDR1-VHFR2-VLCDR3 mimetic with accurate N- to C-terminal sequence, wild-type colicin Ia would not be able to recognize OmpATb (Figure 1G), (c)immunofluorescent dyes showed that OmpATb appeared in the infected lung tissues, even traced the outlines of infected cell membrane and organelles (Figure 4B), (d) PMC-NM molecules selectively interacted with OmpATb, then accumulated in the lesion tissues from circulation (Figure 4B), (e) with immuno-labeling electron microscopic assay, paired 5/10 nm colloid gold molecule images revealed the interaction between OmpATb and PMC-NM molecules at infected host cell membrane (Figure 4D,E), and (f) immunoblotting assay showed PMC-NM recognized the membrane precipitates of the infected lungs, as well as OmpATb of Mtb cells, but did not recognize the precipitates of uninfected and PMC-NM-treated lungs (Figure 1F and 4F).

Early OmpATb studies suggested that OmpATb might act on the outer membrane as a monomer pore (38 kDa)(5, 8). In our immunoblotting assay, the OmpATb precipitations of H37Rv were around 114 kDa, if the interaction with the PMC-NM occurred less than 24 hrs after OmpATb preparation was made, however, they were degraded as 38 kDa precipitations, if the interaction with the PMC-NM occurred beyond 48 hrs. These findings suggest that *in vivo*, at least some part of OmpATb might be in trimmeric form (Figure S3).

Two main domains of PMC-NM are involved in killing Mtb cells, (a) antibody mimetic interacted with OmpATb to drag the channel-forming domain to bind the cell membrane, (b) hydrophobic interaction drove the channel-forming domain to form channel in the cell membrane irreversibly, (c) transmembrane potential opened the channel to induce the leakage of cellular contents resulting in cell death (Figure 4G). Cellular content leakage through the large ion-conductive lumen (9-11 Å) of the colicin channel is a novel mechanism of action against TB cells, as well as infected host cells (9-12,16-19). Either rupture, or shrinkage as empty cell-ghosts occurred in all cells treated

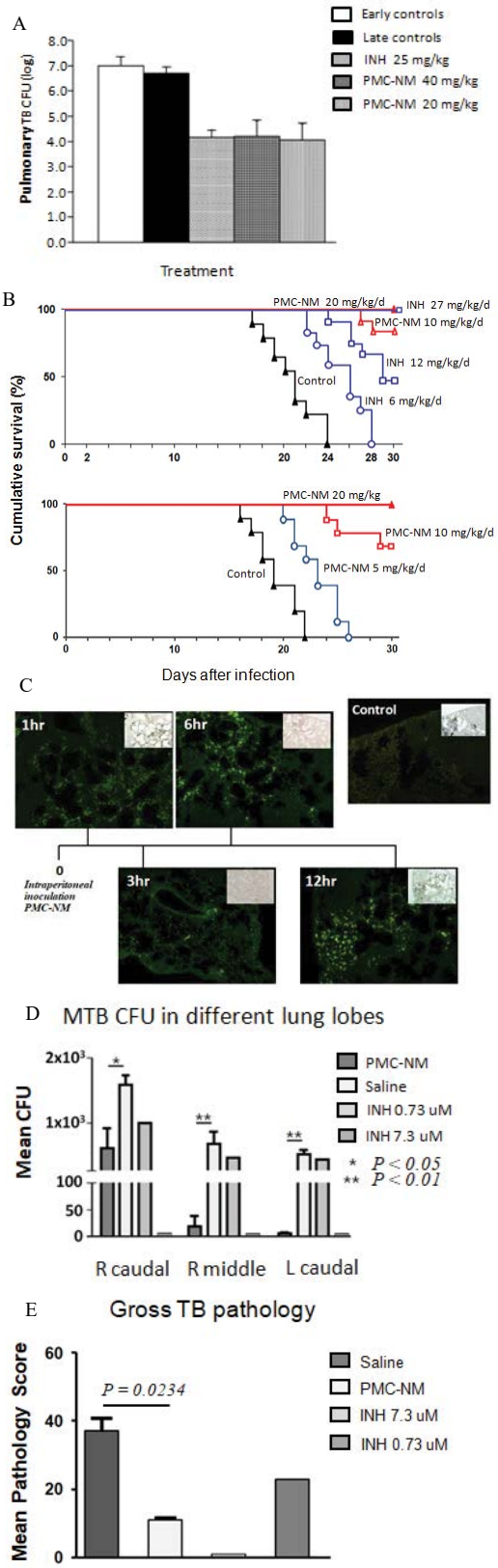

Figure 4: *In vivo* activity of PMC-NM in murine and macaque TB.
(**A**) Mtb CFU of Mtb Erdman infected mice lung after 4-wk treatment with either saline, INH, or PMC-NM. t test was used to determine significant differences between the PMC-NM and saline groups ($p<0.05$), INH and saline groups ($p<0.05$). (**B**) Cumulative survival of MDR-TB (MDR-06005) infected mice with 4-wk injected intraperitonealy (i.p.) with saline, INH 6, 12 mg/kg/d, or PMC-NM 10, 20 mg/kg/d; or with saline, or PMC-NM 5, 10, 20 mg/kg/d. The numbers of surviving mice at various time points were determined, and Kaplan-Meier analysis was used to determine significant differences between the PMC-NM 10, or 20 mg/ml treatment with other treatments ($p<0.05$). (**C**) Immunolabeled PMC-NM molecules (green) selectively accumulated in mice pulmonary MDR-TB lesions at 1 to 12 hrs after one-time i.p. application (40x, inlet, optical images). (**D**) 5-wk i.v. 2 mg/kg/d PMC-NM significantly reduced Mtb H37Rv burdens in macaque lungs. (**E**) PMC-NM significantly controlled macaque gross TB pathology and lesions.

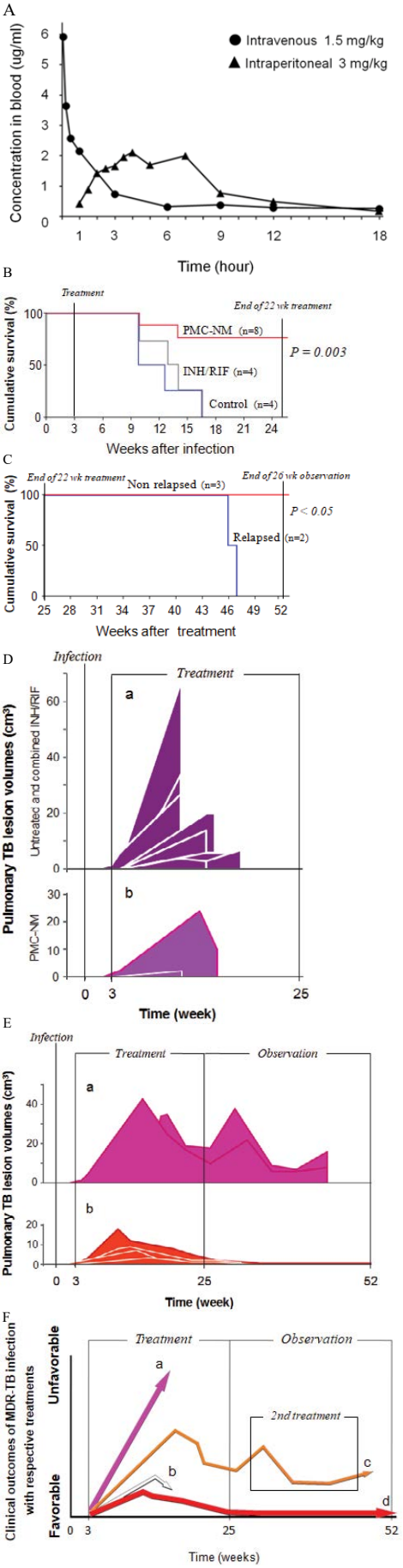

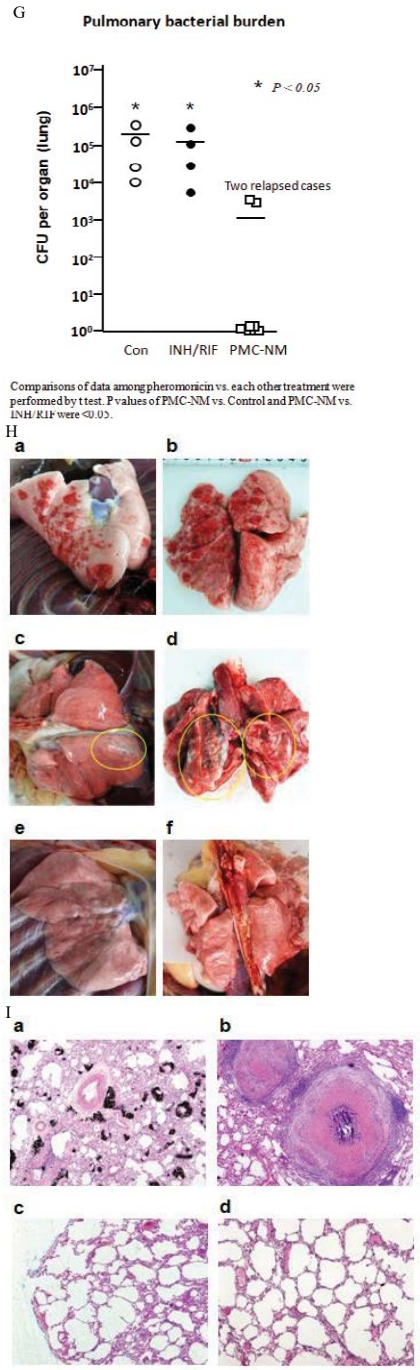

Figure 5: *In vivo* activity of PMC-NM against MDR-TB infection in macaque.
(**A**) Pharmacokinetic assays indicate that i.p. application provided a longer circulatory retention contour. (**B, C**) Cumulative survival of PMC-NM-treated macaques and controls. The numbers of surviving animals at various time points were determined, and Kaplan-Meier analysis was used to determine the significance of difference between the PMC-NM and control groups (*p=0.003*) and the non relapsed and relapsed cases (*p<0.05*). (**D**) Variations of pulmonary TB lesion volumes with different treatments, (**a**) Untreated and INH/RIF, n=8, (**b**) euthanized of PMC-NM, n=2. (**E**) Variations of pulmonary TB lesion volumes with PMC-NM treatment, (**a**) relapsed, n=2, (**b**) non relapsed, n=4. (**F**) The clinical outcomes of respective treatments were extrapolated as the function of D and E variations, (**a**) untreated and INH/RIF treatments; (**b**) euthanized, (**c**) relapsed and (**d**) non relapsed cases of PMC-NM treatment. (**G**) MDR-TB burdens of the whole lung. Each symbol is one macaque. Macroscopic view of lungs of control (**Ha,b**), INH/RIF-treated (**Hc,d**, granulomas, yellow circles) and PMC-NM-treated macaques (**He,f**). Microscopic view of lungs, (**Ia**) Miliary TB dissemination with necrotic mineralization in the lung of untreated controls. (**Ib**) Aggravated granulomas in the lung of INH/RIF-treated controls. Conversely, the lung appearance of PMC-NM treated animals was almost normal at the end of 22-wk treatment (**Ic**), or at the end of 52-wk test (**Id**). (40x, HE staining)

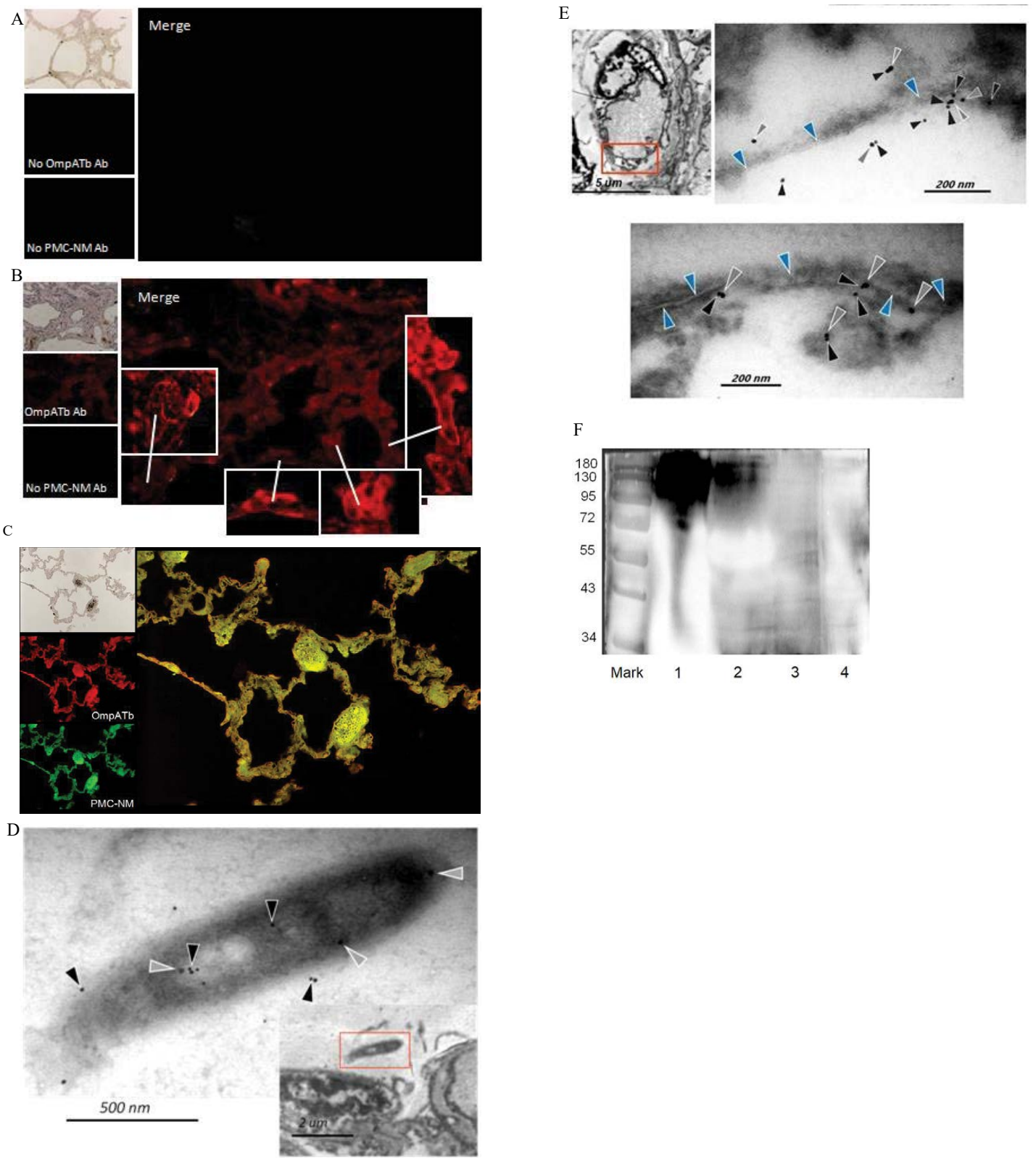

Figure 6: Probably PMC-NM targeting/killing mechanism.

(**A**) Untreated control. (200x) (**B**) OmpATb appeared on cell membranes and organelles of infected host cells (insets).(200x) (**C**) PMC-NM molecules accumulated on the surface of infected host cells through circulation. (200x) (**D,E**) Mtb and Infected host cells were probed with anti-OmpA and anti-PMC-NM Abs with 5 and 10 nm colloid gold molecules (grey and black arrows, respectively). Paired gold molecules revealed the OmpATb/PMC-NM interaction around the cell membranes (blue arrows). Bar, 0.2–1 μm. (inset, the location of higher resolution images). (**F**) Immunoblotting assay showed that PMC-NM interacted with the membrane precipitates of infected macaque lung, as well as OmpATb of Mtb cells, but interacted nothing with the precipitates of uninfected and PMC-NM-treated lungs. Lanes, (**1**) Mtb H37Rv, (**2**) infected lung, (**3**) uninfected lung, (**4**) PMC-NM-treated infected lung.

with PMC-NM (Figure 4H,I). PMC-NM could therefore target/kill any cell, either prokaryocytes, or eukaryocytes, with lipid bilayer cell membranes, if OmpATb appeared on their surface. Future studies will help to further define the specific mechanism of action of PMC-NM.

Comparing with activities of tested standard anti-TB agents, MIC of pan-susceptible Mtb strains/MDR-TB isolates and *in vivo* efficacy indicated that PMC-NM presents a new mechanism of action. Cellular content leakage induced by PMC-NM channels is much more robust, as compared to biochemical activity of standard anti-TB agents which is more easily interrupted through mutagenesis. Present resistance mechanisms of MDR-TB, such as interfering with the binding of drug to target protein, or reducing drug-activating enzymes, presumably were unable to block the activation of PMC-NM channels in the TB cell membrane.

Notably, the MICs of PMC-NM against MDR and XDR Mtb strains were commonly higher than that of against drug-sensitive Mbt strains. The following factors might explain the variance of PMC-NM inhibition concentrations across various clinical and lab strains of Mtb, (a) mutant or other structural alterations of Mtb surface, (b) differential expression of OmpATb by these Mtb strains, or the differential presentation of OmpATb on the surface of infected host cells and (c) functional alteration of antibody mimetic domain of PMC-NM. We will continue related investigation in future studies.

Normal blood biochemical parameters, and lack of weight loss or abnormal behavior indicated that treatment with PMC-NM for 22-wks did not induce evident toxicity (Table 5). PMC-NM *in vivo* bactericidal efficacy against MDR-TB infection indicated that PMC-NM appears to act in the host circulation with full bioactivity.

Additional studies will be necessary to better understand the potential therapeutic efficacy of PMC-NM in multi-drug regimens in combination with anti-TB chemotherapy.

Our data supports the further development of this biological agent and future use with an optimized background regimen against MDR-TB infection in human trials.

Acknowledgment

This work was supported by National Science and Technology Major Projects of New Drugs 2012ZX09103301-024 and 2015ZX09102007-014, National High Technology Research and Development Program of China 2011AA10A214 of Ministry of Science and Technology; Beijing Municipal Science & Technology Commission Z131100002713010 and Z161100000116016 to X-Q.Q. We would like to acknowledge the help and scientific critique of H. Li, G. Zeng and CY. Jiang during the preparation of this manuscript. We would also like to acknowledge the help of HL Ma, SB Liang, TF Liu, WC Wang, JY Tang, F Meng, XC Li and BG Yuan in PMC-NM preparation and animal care.

Author Distribution

X-Q.Q., K-F.C., Z-H.X., X-F.Z., Y. P., C-Y.T., C.S., R-Q.L, and M.C. prepared antibody mimetics and pheromonicin-NM molecules, measured in vitro and in vivo activity; X-D.H., and G-K.O. did CT assays and analysis; X-Q.Q., M.C., S.K., Y-L. Z., and Y.W. designed and organized the study and manuscript.

Competing Interests

All authors declare that they have no conflicts of interest.

Summary

Antibody mimetic interaction with OmpATb initiated the channel formation in target cell membrane, then formed channel led cellular content leakage is a novel mechanism of action against MDR-Tb cells. PMC-NM demonstrated high efficacy against pan-susceptible and MDR-TB strains, suppressed the pulmonary TB burdens in murine/macaque TB models and altered the clinical outcomes in macaque MDR-TB infection. Above *in vivo* efficacy indicated that PMC-NM appears to act in the host circulation with full bioactivity and no evident toxicity. Our data supports the further development of this biological agent and future use against MDR-TB infection in human trials.

Materials & Correspondence Data and material availability: All isolates of MDR-TB are available from China Centers for Disease Control, Beijing (pangyu@chinatb.org). The PMC-NM source and methods are available from Lab. of Biomembrane & Membrane Proteins, West China Hospital, Sichuan University (491607484@qq.com). All CT data are available from Dept. of Radiology, 309 Hospital, Beijing (hxd83405107@163.com).

References

1. S Keshavjee, PE Farmer (2012) Tuberculosis, drug resistance, and the history of modern medicine. *N Engl J Med* 367: 931-936. [crossref]
2. M Zignol, AS Dean, D Falzon, W van Gemert, A Wright, et al. (2016) Twenty years of global surveillance of antituberculosis-drug resistance. *N Engl J Med* 375: 1081-1089. [crossref]
3. J Hoffmann, C Chedid, O Ocheretina, C Masetti, P Joseph, et al. (2021) Drug-resistant TB prevalence study in 5 health institutions in Haiti. *PLos One* 16: e0248707. [crossref]
4. DT Hoagland, J Liu, RB Lee, RE Lee (2016) New agents for the treatment of drug-resistant tuberculosis. *Adv Drug Deliv Rev* 102: 55-72.
5. RH Senaratne, H Mobasheri, KG Papavinasasundaram, P Jenner, EJ Lea, et al. (1998) Expression of a Gene for a Porin-Like Protein of the OmpA Family from Mycobacterium tuberculosis H37Rv. *J Bacteriol* 180: 3541-3547.
6. B Kartmann, S Stenger, M Niederweis (1999) Porins in the wall of Mycobacterium tuberculosis. *J Bacteriol* 181: 6543-6546. [crossref]
7. C Raynaude, KG Papavinasasundaram, RA Speight, B Springer, P Sander, et al. (2002) The functions of OmpATb, a pore-forming protein of Mycobacterium tuberculosis. *Mol Microbiol* 46: 191-201. [crossref]
8. M Niederweis (2003) Mycobacterial porings-new channel proteins in unique outer membranes. *Molecular Microbiol* 49: 1167-1177. [crossref]
9. WL Beatty, DG Russell (2000) Identification of mycobaterial surface proteins released into subcellular compartments of infected macrophages. *Infect Immun* 68: 6997-7002. [crossref]
10. JJ Athman, Y Wang, DJ McDonald, WH Boom, CV Harding, PA Wearsch (2015) Bacterial membrane vesicles mediate the release of Mycobacterium tuberculosis lipoglycans and lipoproteins from infected macrophages. *J Immunol* 195: 1044-1053. [crossref]
11. NG Heatley, HW Florey (1946) An antibiotic from Bacterium coli. *Br J Exp Pathol* 27: 378-390.
12. E Cascales, SK Buchanan, D Duché, C Kleanthous, R Lloubès, et al. (2007) Colicin Biology. *Microbiol Mol Biol Rev* 71: 158-229. [crossref]

13. WA Cramer, JB Heymann, SL Schendel, BN Deriy, FS Cohen, et al. (1995) Structure-function of the channel-forming colicins. *Annu Rev Biophys Biomol Struct* 24: 611-641. [crossref]

14. XQ Qiu, KS Jakes, PK Kienker, A Finkelstein, SL Slatin (1996) Major transmembrane movement associated with colicin Ia channel gating. *JGen Physiol* 107: 313-328. [crossref]

15. PK Kienker, XQ Qiu, SL Slatin, A Finkelstein, KS Jakes (1997) Transmembrane insertion of the colicin Ia hydrophobic hairpin. *J Membr Biol* 157: 27-37.

16. XQ Qiu, MA Riley, in The Bacteriocins: current knowledge and future prospects, R Dorit, SM Roy, MA Riley Eds. (Caister Academic Press, Norfolk, 2016), Chap. 4. Capturing the Power of Van der Waals Zone in the Creation of a Novel Family of Bacteriocin-based Antibiotics 65-80.

17. XQ Qiu, H Wang, XF Lu, J Zhang, SF Li, et al. (2003) An engineered multidomain bactericidal peptide as a model for targeted antibiotics against specific bacteria. *Nat Biotechnol* 21: 1480-1485. [crossref]

18. XQ Qiu, J Zhang, H Wang, GY Wu (2005) A novel engineered peptide, a narrow-spectrum antibiotic, is effective against vancomycin-resistant Enterococcus faecalis. *Antimicrob Agents Chemother* 49: 184-1189. [crossref]

19. XQ Qiu, CY Tong, ZQ Zhong, WQ Wang, YW Zuo, et al. (2013) An engineered multidomain fungicidal peptide against plant fungal pathogens. *Acta Physiologica Sinica* 65: 417-432. [crossref]

20. XQ Qiu, H Wang, B Cai, LL Wang, ST Yue (2007) Small antibody mimetics comprising two complementarity -determining regions and a framework region for tumor targeting. *Nat Biotechnol* 25: 921-929.

21. J van den Elsen, L Vandeputte-Rutten, J Kroon, P Gros (1999) Bactericidal antibody recognition of meningococcal PorA by induced fit. Comparison of liganded and unliganded Fab structures. *J Biol Chem* 274: 1495-1501. [crossref]

22. GP Walsh, EV Tan, EC dela Cruz, RM Abalos, LG Villahermosa, et al. (1996) The Philippine cynomolgues monkey (Macaca fascicularis) provide a new non-human primate model of tuberculosis that resembles human disease. *Nat Med* 2: 430-436. [crossref]

23. D Kaushal, S Mehra, PJ Didier, AA Lackner (2012) The non-human primate model of tuberculosis. *J Med Primatol* 41: 191-201. [crossref]

24. J Zhang, YQ Ye, Y Wang, PZ Mo, QY Xian Y, et al. (2011) *M tuberculosis* H37Rv infection of chinese Rhesus Macaques. *J Neuroimmune Pharmacol* 6: 362-370. [crossref]

25. Macaque H37Rv-infection studies were performed at Center for Primate Biomedical Research, University of Illinois College of Medicine, Chicago (2012-2016) and macaque MDR-TB-infection studies were performed at Institute of Experimental Animal Sciences, Peking Union Medical College (2014-2016) with paid service contracts.

26. DM Lewinsohn, IS Tydeman, M Frieder, JE Grotzke, RA Lines, et al. (2006) High resolution radiographic and fine immunologic definition of TB disease progression in the rhesus macaque. *Microbes Infect* 8: 2587-2598. [crossref]

27. T Zhang, SY Li, KN Williams, K Andries, EL Nuermberger (2011) Short-course chemotherapy with TMC207 and rifapentine in a murine model of latent tuberculosis infection. *Am J Respir Crit Care Med*. 184: 732-737. [crossref]

28. JP Lanoix, F Betoudji, E Nuermberger (2014) Novel regimens identified in mice for treatment of latent tuberculosis infection in contacts of patients with multidrug-resistant tuberculosis. *Antimicrob Agents Chemother* 58: 2316-2321. [crossref]

29. MT Coleman, RY Chen, M Lee, PL Lin, LE Dodd, et al. (2014) PET/CT imagine reveals a therapeutic response to oxazolodinones in macaques and humans with tuberculosis. *Sci Transl Med* 6: 265-274. [crossref]

30. PL Lin, T Coleman, JP Carney, BJ Lopresti, J Tomko, et al. (2013) Radiologic responses in cynomolgus macaques for assessing tuberculosis chemotherapy regimens. *Antimicrob Agents Chemother* 57: 4237-4244. [crossref]

31. J Trias, V Jarlier, R Benz (1992) Porins in the cell wall of mycobacteria. *Science* 258: 1479-1481. [crossref]

32. M Faller, M Niederweis, GE Schulz (2004) The structure of a mycobacterial outer-membrane channel. *Science* 303: 1189-1192.

33. M Niederweis, O Danilchanka, J Huff, C Hoffmann, H Engelhardt (2010) Mycobacterial membranes: in search of proteins. *Trends Microbiol* 18: 109-116. [crossref]

34. M Pavlenok, M Niederweis (2016) Hetero-oligomeric MspA pores in mycobacterium smegmatis. *FEMS Microbiol Lett* 363: fnw046. [crossref]

35. SC Chow, H Wang, J Shao (2007) Sample Size Calculation in Clinical Research (Chapman & Hall/CRC, New York, ed. 2, 2007) 5: 121-123.

Citation:

Qiu XQ, Cao KF, Xiong ZH, Zhang XF, Pang Y, et al. (2024) Pheromonicin: A Novel Antimicrobial Inhibited Fatal Multidrug-Resistant M. tuberculosis Infection in Animal Models. *Microbiol Immunol Pathol* Volume 5(2): 1-19.

Supplementary Figures

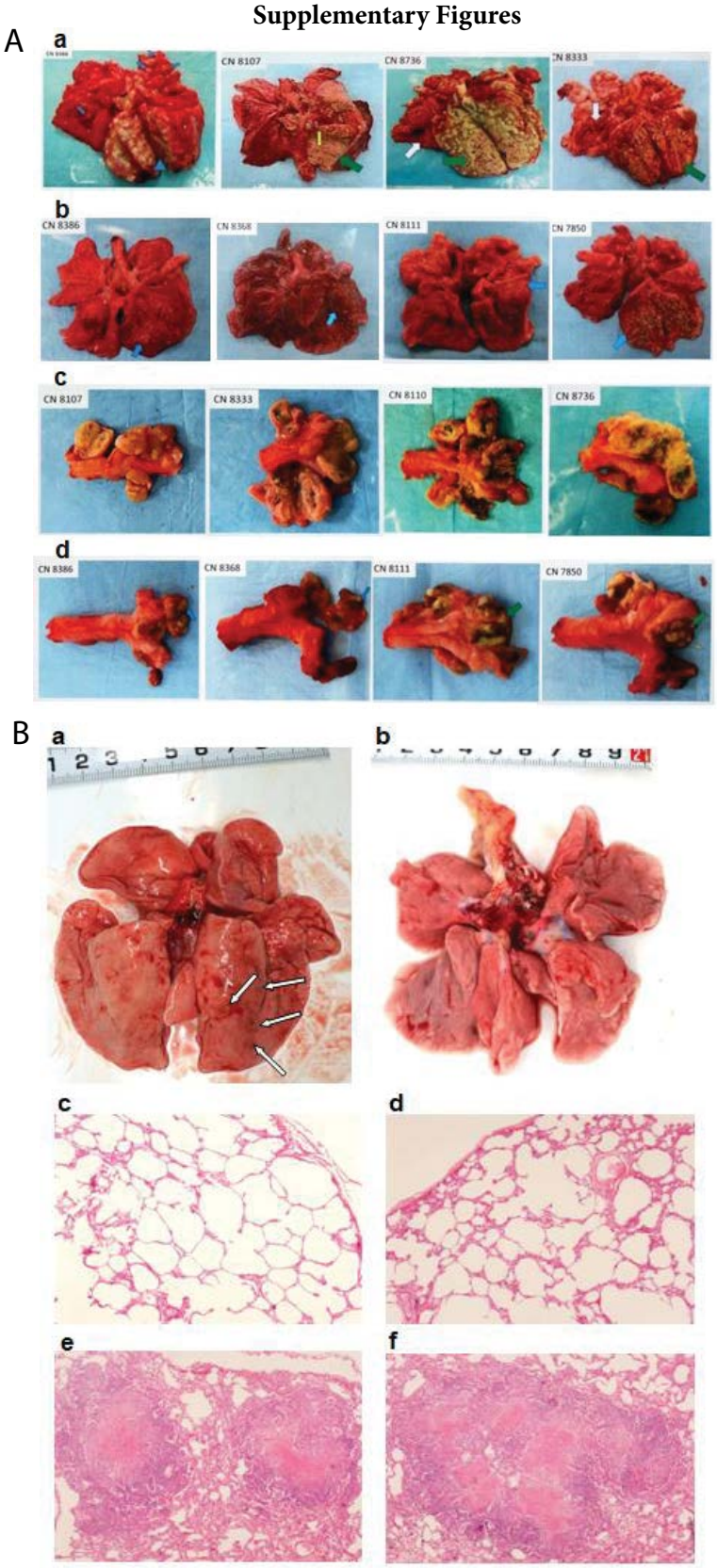

Supple Figure 1: (**A**) Macroscopic views of Mtb H37Rv lesions in macaque lungs, (**a**) Saline-treated and 0.1 mg/kg/d INH-treated controls showed severe TB lesions. (**b**) Most PMC-treated macaques exhibited only small, focal granulomas in the right caudal lobe (infection site), with no or very few disseminated granulomas in other lung lobes. (**c**) Enlarged hilar lymph nodes with caseating necrosis in saline-treated controls. (**d**) Milder changes in hilar lymph nodes of the PMC-NM-treated group. (**B**) Pilot tested macaques were treated as untreated (n=4), or PMC-NM (3 mg/kg/d, i.p.,n=4)at day 3 after infection. Macroscopic view of lungs of control (**a**) and PMC-NM-treated (**b**) macaques. Interstitial cell infiltration were seen in the lungs of PMC-treated macaques (**c,d**) while granulomas were scattered in the lung of controls (**e,f**)(40 x, HE staining).

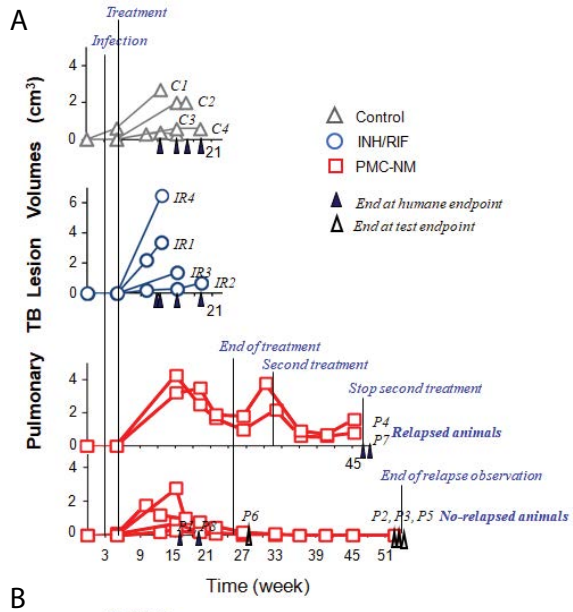

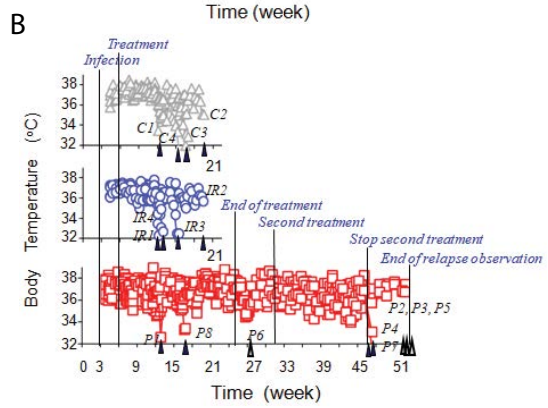

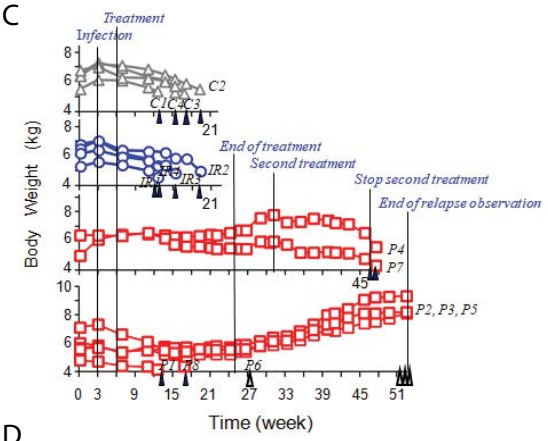

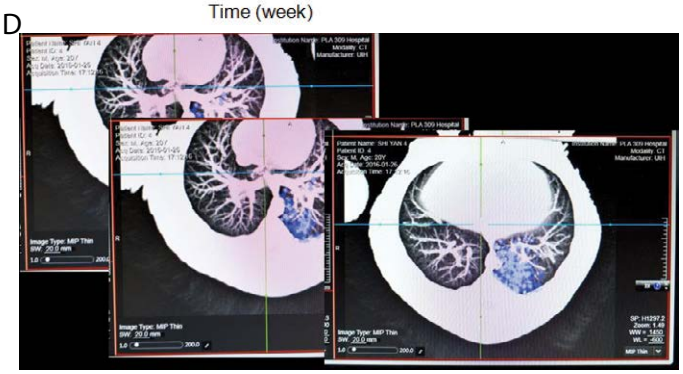

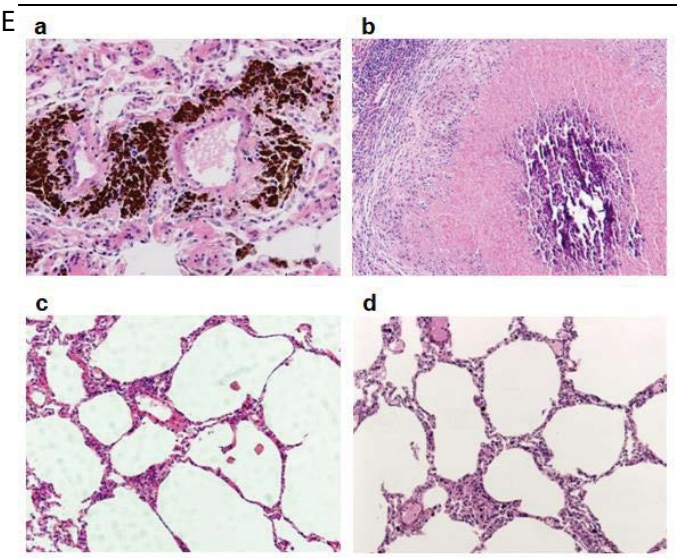

Supple Figure 2: (**A**)Variations in pulmonary TB lesion volumes, body temperature (**B**), body weight (**C**) of PMC-NM-treated macaques in 22-wk treatment and subsequent 26-wk observation period. (**D**) Pulmonary TB lesion volumes were derived from serial CT scans with computerized conversion. (**E**) Microscopic views of pulmonary TB histopathology, (**a**) untreated, (**b**) INH/RIF treatment, (**c**) PMC-NM treatment at end of treatment, (**d**) PMC-NM treatment at end of whole test. 200x, HE-staining.

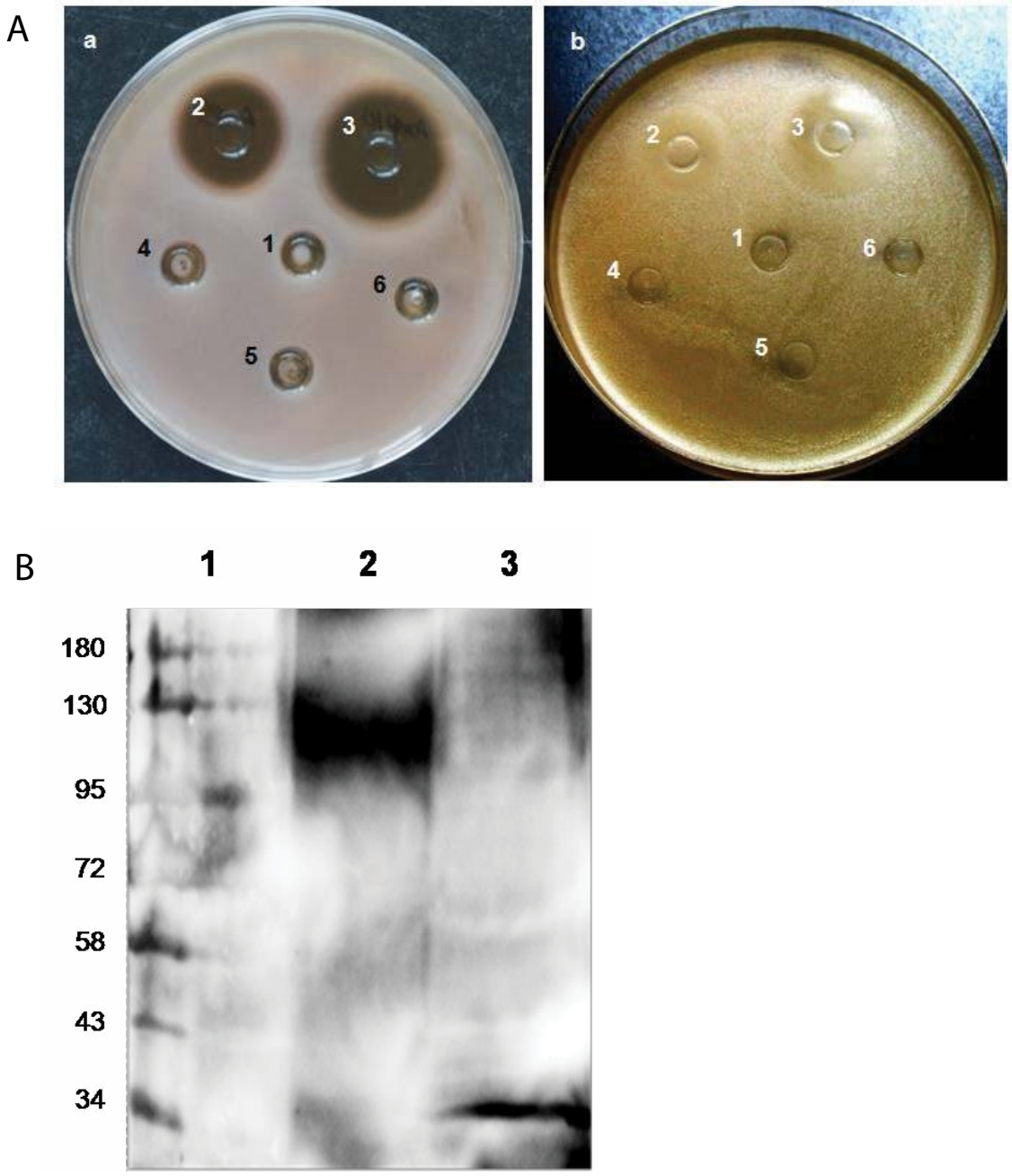

Supple Figure 3: (**A**)PMC-NM has no efficacy to inhibit the growth of (a) *Bifidobacterium longum* and (b) *Lactococcus lactis.* In contrast, ampicillin (amp) inhibited the growth of two probiotics. (1) control, (2) amp 5 ug/ml, (3) amp 10 ug/ml, (4) PMC-NM 2 ugml,(5) PMC-NM 5 ug/ml, (6) PMC-NM 10 ug/ml. (**B**)Time effect of H37Rv OmpATb precipitations. 1. Mark, 2. OmpATb preparation was interacted with PMC-NM less than 24 hrs after OmpATb preparation was made, 3. preparation was interacted with PMC-NM beyond 24 hrs after OmpATb preparation was made.